

1 **Methods for handling redox-sensitive smectite suspensions**

2 **Joseph W. Stucki^{1§}, Kai Su^{1,2}, Linda Pentráková^{1,3}, and Martin Pentrák^{1,3}**

3 ¹Department of Natural Resources and Environmental Sciences, University of Illinois, Urbana,
4 Illinois, USA

5 ²Southwest Jiaotong University, Chengdu, China

6 ³Institute of Inorganic Chemistry, Slovak Academy of Sciences, Dúbravská cesta 9, 845 36
7 Bratislava, Slovakia

8 [§]Corresponding author: W-321 Turner Hall, 1102 S. Goodwin Avenue, Urbana, IL, 61801, USA
9 e-mail: jstucki@illinois.edu

10 11 **ABSTRACT**

12 For handling and storage of redox-sensitive smectites, a controlled atmosphere liquid exchange
13 (CALE) apparatus and glove box were used. For this purpose a fine fraction of Na⁺-SWa-1
14 ferruginous smectite was used in this work. Reduction of structural Fe was conducted with
15 sodium dithionite and buffered by sodium citrate-sodium bicarbonate (C-B) solution at 70 °C for
16 4 h. Changes in color from yellow-brown of unreacted through green-yellow (partially reduced)
17 to dark grey (totally reduced) were observed. A series of prepared samples were washed with de-
18 oxygenated NaCl solutions without contact with oxygen, which could lead to re-oxidation.
19 Another series of samples were washed with NaCl solutions with higher oxygen content. Higher
20 efficiency and suitability of the CALE apparatus for O₂ sensitive clay redox systems was
21 demonstrated. It was more effective in reaction products removal and maintaining of higher Fe

22 reduction. Analysis of solid phases by 1, 10-phenanthroline method provided a high conversion
23 level (91.129 ± 0.477 % of Total Fe %).

24 **KEY WORDS:** nontronite, iron, reduction, re-oxidation, controlled atmosphere liquid exchange
25 apparatus, glow box, centrifuge,

26

27 INTRODUCTION

28 Accurate research in all fields of investigation requires precise tools and techniques to
29 eliminate errors as much as possible. This is especially true for materials (solid, liquid, and/or
30 gaseous) that can be modified by exposure to the natural environment (O₂, humidity,
31 temperature, pressure, UV radiation, etc.) during their sampling, handling, analysis, and storage.
32 Redox-sensitive clay minerals certainly fit within this category.

33 In general, the reduction of Fe(III) to Fe(II) in Fe-rich smectites is now well known
34 (Stucki, 2006, 2013) and has been the aim of numerous investigations over about four decades
35 (Rozenon and Heller-Kallai, 1976; Stucki and Roth, 1977; Russell *et al.*, 1979; Stucki *et al.*,
36 1984a; Wu *et al.*, 1989; Komadel *et al.*, 1990, 1995, 2006; Stucki and Tessier, 1991; Manceau *et*
37 *al.*, 2000; Stucki *et al.*, 2002; Hofstetter *et al.*, 2003; Merola *et al.*, 2007; Schaefer *et al.*, 2011;
38 Hofstetter *et al.*, 2008; Neumann *et al.*, 2008; Dong *et al.*, 2009; Neumann *et al.*, 2009; Gorski
39 *et al.*, 2011; Neumann *et al.*, 2011; Alexandrov *et al.*, 2013), and others). This phenomenon has
40 also been investigated and described as it relates to both biological (Stucki *et al.*, 1987; Kostka *et*
41 *al.*, 1999; Dong *et al.*, 2003, 2009; Li *et al.*, 2004; Jaisi *et al.*, 2005, 2007; O'Reilly *et al.*, 2005,
42 2006; Kukkadapu *et al.*, 2006; Lee *et al.*, 2006; Zhang *et al.*, 2007; Ribeiro *et al.*, 2009;
43 Pentráková *et al.*, 2013) and environmental (Peretyazhko *et al.*, 2008; Jaisi *et al.*, 2009; Neumann

44 *et al.*, 2009; Zhang *et al.*, 2009; Cervini-Silva *et al.*, 2010; Bishop *et al.*, 2011; Southam, 2012;
45 Zhuang *et al.*, 2012) processes.

46 An understanding of these phenomena over the past decades came about because of the
47 development of methods and apparatus which preserve the oxidation state of the structural Fe
48 during preparation and analysis of the samples. The need for these methods was recognized by
49 Stucki (1975) while attempting to confirm the oxidation-reduction mechanism for structural Fe
50 in smectites proposed by Roth *et al.* (1969) and Roth and Tullock (1972), which was based on
51 the belief that no change in layer charge occurred during reduction of the structural Fe. By
52 protecting the sample from atmospheric O₂ during measurements of cation exchange capacity,
53 however, Stucki and Roth (1977) showed a definitive increase in layer charge with increasing
54 structural Fe(II), but that the increase was not a linear function of the extent of reduction. The
55 methods and apparatus used in those studies were described briefly by Stucki *et al.* (1984a), but a
56 complete and detailed description has never been given, especially one that includes how they
57 have evolved and been improved through the years. This is the purpose of the present
58 publication.

59 For correct characterization of such materials, they must be sampled, handled, and
60 analyzed under conditions which prevent or minimize re-oxidation. Described below are
61 laboratory methods and apparatus that accomplish these aims, and include methods for chemical
62 reduction, removal of excess salts, addition of O₂-free reactants, drying, sample transfer, storage,
63 and analysis by chemical and spectroscopic methods.

64

65 **MATERIALS AND METHODS**

66 **Materials**

67 Redox-protective methods were illustrated and tested using ferruginous smectite (sample
68 SWa-1 from the Source Clays Repository of The Clay Minerals Society) as the example clay
69 mineral submitted to a chemical reduction process which included various steps of washing and
70 freeze drying. The sample was fractionated ($<2\ \mu\text{m}$), Na^+ -saturated, and freeze dried before use
71 and labeled Na-SWa-1 (Stage 0, Figure 1). All chemicals used were analytical-reagent grade,
72 except sodium dithionite was technical grade. The supplier of all chemicals was Thermo-Fisher
73 Scientific (Pittsburgh, Pennsylvania). Citrate-bicarbonate (C-B) buffer solution was prepared by
74 combining 24 parts of 1.0 M sodium bicarbonate and 1 part of 0.9 M sodium citrate. All water
75 used was purified to a resistivity of approximately 18 M Ω -cm and is referred to hereafter as
76 DI water.

77 **Methods**

78 *O₂-free gas*

79 Oxygen-free gas was obtained by passing standard Ar gas through a hot (130 °C) O₂ trap
80 (Chromatography Research Supplies (CRS), Louisville, Kentucky, ¼-inch Model 1000 [or older
81 bugle-shaped version] high-capacity O₂ trap with 500 cm³ of Cu/Zn/Al catalyst) wrapped with
82 heating tape and covered with aluminum foil. Valves were installed at both ends of the trap. The
83 purge gas could be N₂ (less expensive than Ar) if permitted by the objectives of the study. In the
84 authors' laboratory, Ar was selected over N₂ because some target analyses were for species of N.
85 The CRS Model 1000 O₂ trap has a capacity of 2.5 L of O₂ at room temperature and **xx** L at 130
86 °C.

87 Once spent, the catalyst in the trap required regeneration. This was accomplished by pre-
88 heating it to 130 °C then purging with N₂ for 15 min at a flow rate of 50 cm³/min. The purge gas
89 was then changed to a mixture of Ar + 10% H₂, the temperature raised to 300 °C, and the flow

90 rate increased to 350 cm³/min. The trap was then held under these conditions for 4 h. The
91 effluent gas was vented into a hood. Water formed as the H₂ reacted with adsorbed O₂, and the
92 inert gas swept the water vapor from the trap. When regeneration was complete, no more water
93 vapor could be detected in the gas stream. The outlet valve to the trap was then closed and the
94 line at that end disconnected. The power was turned off to allow the trap to cool under
95 regenerating gas pressure. When the trap reached room temperature, the input valve was closed
96 and the trap was disconnected from the regeneration gas input line and reinstalled at the site of
97 application.

98 To reinstall the O₂ trap at the application site without exposing the catalyst to the
99 atmosphere or contaminating the inert-gas supply with atmospheric O₂, the following procedure
100 was used. First, all valves in the inert-gas supply line downstream from the main gas valve on the
101 cylinder and between it and the O₂ trap were opened to the atmosphere and the line was
102 disconnected at the inlet end of the trap. Second, the main gas valve on the cylinder was opened
103 to sweep all atmospheric gases away from the main cylinder supply. Third, the flowing stream of
104 the inert input gas was flooded over the input connector to the trap, which was then connected
105 and tightened while the gas was flowing. Fourth, the input valve to the trap was opened. Fifth,
106 the heating tape around the trap body was energized to raise the catalyst temperature to 130 °C.
107 Sixth, the output valve was not opened until needed to purge the target apparatus. This sequence
108 is designed to minimize the contamination of the inert gas supply and to extend the life of the
109 catalyst in the trap.

110 *Apparatus for handling Fe-reduced clay*

111 Fundamental to the investigation of redox-modified smectites is an inert-atmosphere
112 reaction tube (IRT), which consisted of a centrifuge tube and septum-sealing cap (Figure 1A) in

113 which the clay mineral sample was dispersed, reduced, washed, and reacted with desired
114 chemical solutions. It was designed so that the dispersion could be accessed using septum-
115 penetration needles (6 inch, 22 gauge, deflected point), which enabled solution manipulations
116 without exposure to the atmosphere. For this purpose, a 50-mL polycarbonate, round-bottom,
117 Oak Ridge type centrifuge tube was chosen (Figure 1A, 17), such as Thermo-Fisher catalog
118 number 3118-0050. It has the advantages of chemical resistance, transparency, and reasonable
119 volume. A septum-sealing cap to fit this centrifuge tube was designed with three parts: (1) a rigid
120 teflon disc with o-ring (such as Thermo-Fisher catalog number DS3131-0024) and a 0.25-inch
121 diameter center hole (hand drilled in the laboratory) (Figure 1A, 15), which was placed on the
122 opening of the centrifuge tube such that the o-ring sealed against the lip of the tube when
123 tightened; (2) a septum disc (Figure 1A, 14) cut from a Pursep T[®] septum sheet (catalog number
124 230696, Chromatography Research Supplies, Louisville, Kentucky, USA, [describe septum
125 materials here]), using a 1-inch diameter, hollow-cylinder cutter (such as a cork borer), which
126 was then placed across the opening of the centrifuge tube, supported by the rigid teflon disc; and
127 (3) an Al cap (Figure 1A, 13), also drilled with a 0.25-inch center hole, to compress and seal the
128 septum and septum support onto the centrifuge tube. All pieces were designed to fit inside a
129 Dupont/Sorvall model SS-34 centrifuge rotor or equivalent.

130 The septum-penetration needles used to gain access into the IRT were attached to the
131 sampling port of a controlled-atmosphere liquid exchanger (CALE) (Figure 2). The sampling
132 port was connected to various condenser flasks containing degassed solutions, which could be
133 individually selected, through a carefully orchestrated network of valves and tubing (Figure 2).
134 The CALE used in the authors' laboratory contained four flasks in which four different solutions
135 could be deoxygenated before being selected for solution transfer into the IRT.

136 Each condenser flask in the CALE was a modified 2-L flat bottom flask (Figure 1B, 2) to
137 which four equally spaced vertical ports were added using ACE-Threds glass risers to accept
138 0.25-inch glass tubing. Sealed access to the inside of the flask was gained through these ports for
139 a gas dispersion tube (Figure 1B, 8), which was slightly curved away from the flask wall; a
140 solution withdrawal tube (Figure 1B, 7), which was also slightly curved; a short tube connecting
141 the flask atmosphere to vacuum (Figure 1B, 6); and another short tube leading to a 10-psi
142 pressure relief valve (Figure 1B, 5). A 1-inch, magnetic stirring bar was placed in the bottom
143 (Figure 1B, 3). The center neck of the flask was a 2.5-inch o-ring joint (such as on the Ace Glass
144 8273 adapter), designed to mate with the condenser column and cooling coil assembly above it.

145 The lower portion of the condenser column consisted of a solution cooling coil (Figure
146 1B, 4) which was sealed to the center neck of the flask (Figure 1B, 4) using a metal clamp
147 (Figure 1B, 13) around the 2.5-inch o-ring joint (Figure 1B, 9). When in place, the cooling coil
148 extended downward into the solution as far as possible without interfering with the stirring bar.
149 The inlet to the coil was connected to a cold-water source and the outlet to a sink drain. At the
150 top of the cooling coil was a female, 1-inch, standard-taper, ground-glass joint designed to
151 receive the condenser column (Figure 1B, 11) above it. The joint was sealed using a thin film of
152 vacuum grease and held in place with corrosion-free wire springs (7600 Stainless steel Clamp,
153 for joint of size 24/40, ACE Glass catalog number: 7600-25) (Figure 1B, 10).

154 The condenser column (Figure 1B, 11) consisted of a coiled glass tube that was open to
155 the flask at the bottom and housed inside a water jacket through which cold water was circulated.
156 The top of the coiled tube was connected to a 4-position stopcock which enabled the solution
157 inside the flask to be completely isolated from the atmosphere (position 1), open to the
158 atmosphere (position 2), open to a source of O₂-free gas (position 3), or simultaneously open to

159 both the atmosphere and the O₂-free gas (position 4). In this last position, the O₂-free gas was
160 continuously swept across the top of the condenser column, which maintained an open system at
161 atmospheric pressure inside the flask without permitting O₂ to enter back through the column
162 (Figure 1B, 12).

163 The access ports to the condenser flasks in the CALE were connected to a distribution
164 network (Figure 2) through a series of tubes and valves which were operated in concert with each
165 other in various combinations. The valve combinations, together with appropriate settings for the
166 stirrer hot plates, were defined to achieve the specific purposes of the apparatus (see the various
167 Configuration definitions in Table 1). The two major inputs for the network were O₂-free Ar and
168 vacuum, and within the network the principal activities were to deoxygenate the flask solutions
169 and to transfer them and supernatant solutions into or out of the IRT through the sample port.

170 The CALE (Figure 2) was prepared with deoxygenated 1 M and 0.005 M solutions of
171 NaCl in flasks 1 and 2, respectively, and with deoxygenated DI water in flask 4. The solution in
172 flask 3 varied depending on the needs of the experiment. For example, when testing the nitrate
173 reduction capacity of a redox-modified smectite (Su et al., 2012), flask 3 was filled with 0.001 M
174 NaNO₃. To fill the respective flasks, a volume of 1 to 2 L of the desired solution was prepared in
175 an Erlenmeyer flask or beaker and then connected to the sample port of the CALE through a
176 flexible tube which replaced the needle. Configuration I (Table 1) was then employed to siphon
177 the desired solution into its flask. The solution was then deoxygenated by changing to
178 Configuration II, boiling for 1 h with O₂-free gas flowing, then cooled to room temperature using
179 Configuration III in which cold water was circulated through the cooling coil to effect rapid
180 cooling of the solution after the de-oxygenation heating cycle. This cooling coil is not required,
181 but shortens the time needed for cooling. Supernatant solution was removed from the IRT using

182 Configuration V (supernatant discarded or saved), and the selected deoxygenated solution was
183 transferred to the sample IRT using Configuration VI. Configuration IV was the regime used to
184 store solutions in all flasks after de-oxygenation or when in standby status. Other actions were
185 also possible as defined by the other Configurations (Table 1).

186

187 *Preparation stages of the Fe-reduced smectite*

188 To test the effectiveness of these apparatus in protecting the sample from atmospheric O₂,
189 a 50-mg portion of freeze-dried Na-SWa-1 was dispersed in 20 mL of DI water inside the IRT by
190 shaking overnight, then 10 mL of C-B buffer solution was added, the septum-sealing cap re-
191 installed, and the suspension mixed thoroughly using a vortex mixer. This process is referenced
192 **JWS Here** hereafter as “resuspension in C-B buffer” (Stages 1 and 5, Figure 1).

193 Reduction of structural Fe in the sample was accomplished by first preheating the sample
194 to 70°C in a water bath, then inserting two needles through the septum. The first needle (6 inch,
195 22 gauge, deflected point) supplied O₂-free Ar gas to the bottom of the dispersion and the rising
196 bubbles effected continuous gentle mixing; the second (2 inch, 22 gauge, deflected point) served
197 as a vent to allow Ar to escape from the head space above the dispersion without permitting a
198 back flow of atmospheric O₂. The deflected point design was chosen in order to minimize coring
199 of the septum by the needle. Once the gas flow was established in the IRT and the sample was at
200 temperature, the septum-sealing cap was removed briefly while 200 mg of granular sodium
201 dithionite was added, then the cap was re-installed. The reduction reaction proceeded for 4 h at
202 70 °C, after which the tubes were removed and cooled at room temperature for 1 h with the Ar
203 gas continuing to purge the vessel. This time and temperature were selected because Komadel et
204 al. (1990) found these to be effective in achieving maximum reduction of the structural Fe.

205 Lesser levels of reduction can be achieved by decreasing the time (Lee et al, 2006; Ribeiro et al.,
206 2009), temperature (Komadel et al., 1990), and/or amount of sodium dithionite added (Komadel
207 et al., 1990).

208 In one experiment, the reduction process was monitored continuously by UV-Vis
209 spectroscopy by using a modified version of the IRT (Figure 3) in conjunction with a quartz flow
210 cell (Cary Q6, Part No. 6610015200) and a peristaltic pump (Masterflex[®] C/L[®] Dual-Channel
211 Variable-Speed Tubing Pump, model R-77120-52). The modified IRT (Figure 3) consisted of a
212 50-mL glass centrifuge tube with the same screw cap as in Figure 1. The body of this centrifuge
213 tube was enclosed inside a water jacket (Figure 5) which was connected to Tygon LFL tubing
214 (Tube ID 2.79 mm, R-96429-48) for water and sample circulation by the dual-channel peristaltic
215 pump. The glass reaction vessel (Figure 3, 5) was closed at the top using the septum-sealing cap
216 (Figure 3, 1). Two needles were then inserted into the vessel (Figure 3, 6 and 7) to establish an
217 open system while maintaining an inert atmosphere, as described for sample reduction above.
218 The water circulating in the jacket was taken from the water bath at 70 °C, and the sample was
219 circulated through a quartz flow cell located in the beam path of the spectrophotometer. After
220 about 10 min of temperature equilibration of the Na-SWa-1 suspension with the water bath, a
221 reference spectrum was obtained from 200 to 800 nm, then the wavelength was fixed at 730 nm
222 and continuous recording of the absorbance value at this wavelength was begun. The screw cap
223 was opened and approximately 200 mg of sodium dithionite was added. At selected intervals, the
224 spectrum was scanned from 200 to 800 nm then returned to a fixed value of 730 nm.

225 ***Removing excess salts from redox-activated Na-SWa-1***

226 Converting samples into suitable forms for analysis usually requires the removal of
227 reaction products and other solutes (e.g. citrate, bicarbonate, excess NaCl, dithionite degradation

228 products, etc.) associated with the reduction reaction, and minimizing the concentration of
229 solutes in the outer solution of the dispersion. This was accomplished by centrifuge washing
230 (Sorvall Dupont Model RC4-M Plus centrifuge with SS-34 rotor) at 1400 x g (3000 rpm)
231 **[Martin, are these numbers correct? Shouldn't the g force be greater than the rpm?].**

232 If the supernatant remained cloudy, the g force was doubled. During this washing
233 procedure, supernatant solutions were decanted and discarded using Configuration V of the
234 CALE, as described above, with the first needle (6-inch, 22 gauge, deflected point) inserted into
235 the supernatant to a point just above the sediment (down location, Table 1) and the second needle
236 (6-inch, 22 gauge, deflected point) inserted into the head space (up location, Table 1).
237 Supernatant was withdrawn by vacuum into the discard container and a positive pressure was
238 maintained inside the vessel by Ar addition. New solution was then added using Configuration
239 VI. Sample re-dispersion was accomplished by vortex mixing, vigorous shaking, and/or bath
240 sonication for 15 min, depending on the agglomeration in the sample. Vortexing while slowly
241 refilling helps the redispersion process. These steps allowed the exchange of solutions in the IRT
242 without exposing the redox-activated Na-SWa-1 to atmospheric O₂. The initial supernatant
243 solution was replaced with 1 M NaCl from flask 1; followed by three to five more washings with
244 0.005 M NaCl from flask 2. These washing steps used 1400 x g for 20 min. After decanting in
245 the last washing step, another solution (from flask 3 or 4) or nothing was added, depending on
246 the experiment.

247 *Glove-box handling and storage*

248 A glove box with antechamber (Vacuum Atmospheres Model HE-4), equipped with a
249 Pedratol automatic pressure-control system and a dry train through which the N₂ or Ar
250 atmosphere was continuously circulated to remove H₂O and O₂ was used to store some samples,

251 to transfer samples to some types of holders, and to freeze dry the sample under an inert
252 atmosphere (Figure 4).

253 Freeze drying capability under an inert atmosphere was added to the inside of the glove
254 box by installing a vacuum valve and tubing and a thermoelectric cold plate (model CP-2,
255 Thermoelectric Unlimited, Inc., Wilmington, Delaware) The cold plate was equipped to hold and
256 freeze the contents of up to 4 IRTs simultaneously (Figure 4, 2). A special cap was manufactured
257 to replace the sealing-cap assembly and to connect the IRT to the vacuum line (Figure 4, 4).
258 When in place, this cap securely isolated the evacuated IRT atmosphere from the glove-box
259 atmosphere, thus preventing the applied vacuum from lowering the pressure inside the glove
260 box. Once the sample was securely frozen, the vacuum valve was opened and the atmosphere
261 within the IRT was then continuously evacuated to sublime the frozen H₂O from the sample gel.

262

263 *Stages for Analyzing Reduced Na-SWa-1*

264 Reduced samples were then investigated at certain stages of the chemical reduction and
265 washing processes in order to assess the reliability of the inert-atmosphere handling methods.
266 These stages were (Figure 1):

267 Stage 0: Freeze-dried, Na-saturated, <2- μ m particle-size fraction of ferruginous
268 smectite (labeled Na-SWa-1).

269 Stage 1: Freeze-dried, Na-SWa-1 from Stage 0, resuspended in C-B buffer.

270 Stage 2: Freshly reduced Na-SWa-1 in suspension prior to any washing or further
271 treatment.

272 Stage 3: A compressed gel obtained by centrifuging the suspension in Stage 2 at
273 35,000 x g (20,000 rpm) and decanting the supernatant.

274 Stage 4: Freeze-dried form of the reduced, unwashed sample from Stage 3, using
275 the freeze dryer inside the glove box.

276 Stage 5: Resuspension of freeze-dried sample from Stage 4 with C-B buffer.

277 Stage 6: Washed (5X) samples from Stage 2 (A, washed with CALE; B, washed
278 without CALE) or Stage 5 (C, washed with CALE). Washing was with a 5 mM NaCl or
279 H₂O solution and left in suspension after the final wash.

280 Stage 7A, 7B, 7C: A compressed gel obtained by centrifuging the respective
281 suspensions in Stage 6 at 35,000 x g (20,000 rpm) and decanting the supernatant.

282 Stage 8A, 8B, 8C: Freeze-dried form of the reduced, compressed gels from Stages 7A,
283 7B, 7C, respectively..

284

285 ***Chemical Analysis for Structural Fe Reduction***

286 The reduced state (Fe(II) content) of the smectite was determined in either the gel or
287 freeze-dried state using the 1,10-phenanthroline method (Komadel and Stucki, 1988). The
288 septum-sealing cap was removed from the IRT containing the sample in either Stage 4 or 5, then
289 12 mL of 3.6 N H₂SO₄, 2 mL of 10% (w/v) 1,10-phenanthroline in 95 % ethanol, and 1 mL of
290 48 % HF were added immediately, in that order, under red lights. These solutions were not
291 purged of O₂ because the low pH prevented oxidation of the tris(1,10-phenanthroline)Fe(II)
292 complex. The open tubes were heated for 30 min in a boiling water bath and cooled for 15

293 minutes at room temperature. To remove excess F⁻, 10 mL of 5% (w/v) H₃BO₃ was added. The
294 solutions were then diluted as prescribed by the method (Stucki, 1981; Stucki and Anderson,
295 1981; Komadel and Stucki, 1988), and analyzed for Fe(II) at 510 nm (Varian Cary 5E UV-Vis-
296 NIR spectrophotometer). Total Fe was measured after exposing the diluted samples to ultra-
297 violet light for 2 h. For freeze-dried samples (Stage 5), the amount of Fe(II) and total Fe were
298 calculated from the Beer-Lambert Law, *viz.*,

$$A_i = \epsilon_i l C_i \quad [1]$$

299 where *i* refers to either Fe(II) or total Fe, *A_i* is the absorbance at 510 nm of either the Fe(II) or
300 total Fe solution, ϵ_i is the absorbance of the 1,10-phenanthroline Fe(II) complex in the Fe(II) or
301 total Fe solution (0.1836 and 0.1921 g/μg-cm for Fe(II) and total Fe, respectively), *l* is the path
302 length (exactly 1.00 cm for all analyses), and *C_i* is the concentration of Fe(II) or total Fe (μg/g)
303 in the analyte solution.

304 For samples analyzed while in the undried gel state (Stage 4 or 7), the exact amount of
305 starting material was unknown, so only the ratio of Fe(II)/Total Fe $\left(\frac{C_{Fe(II)}}{C_{Total}} \right)$ could be
306 determined, which was calculated from Equation 2, using the ratios of absorbance values

307 $\left(\frac{A_{Fe(II)}}{A_{Total}} \right)$ from Equation 1.

$$\frac{C_{Fe(II)}}{C_{Total}} = \frac{A_{Fe(II)} \epsilon_{Total}}{A_{Total} \epsilon_{Fe(II)}} \quad [2]$$

308 ***Mössbauer Spectroscopy***

309 Mössbauer spectra were collected using a Web Research, Inc. (Edina, Minnesota),
310 spectrometer equipped with a Janis model SHI-850-5 (Janis, Inc., Wilmington, Massachusetts)
311 closed cycle cryostat and operating in triangle waveform mode with a 50 mCi ^{57}Co source
312 dispersed as 10 wt.% in a thin Rh foil, obtained from Ritverc, Inc (St. Petersburg, Russia). The
313 velocity scale was calibrated using the magnetic hyperfine field (B_{hf}) of a 7 μm thick $\alpha\text{-Fe}$ foil at
314 the sample temperature. To estimate the correct value for B_{hf} at 77 K, Mössbauer spectra of the
315 alpha Fe were collected at 4, 77, and 298 K, then the number of channels separating peaks 1 and
316 6 were plotted as a function of temperature. Values for B_{hf} for $\alpha\text{-Fe}$ at 4 and 298 K were
317 determined by Violet and Pipkorn (1971) to be 33.9 T and 33.1 T, respectively. The
318 corresponding value at 77 K was found to be the same as at 4 K, i.e. 33.9 T, so this value was
319 used to calibrate the velocity scale.

320 RESULTS AND DISCUSSION

321 The effectiveness of these methods and apparatus for preserving the oxidation state
322 during the preparation, handling, and storage of redox-sensitive ferruginous smectite samples
323 was tested in several ways. First, the color was monitored, both by eye and spectroscopically.
324 Second, the structural Fe(II) content was measured chemically, either gravimetrically or as a
325 ratio of Fe(II) to total Fe, using the 1,10-phenanthroline method. And third, the extent of
326 reduction and structural alteration was assessed using Mössbauer spectroscopy with the sample
327 at 77 K.

328 **Color**

329 Unreduced and reduced Na-SWa-1 samples differed markedly in their color, as is well
330 known (Roth and Tullock, 1973; Rozenson and Heller-Kallai, 1976; Stucki and Roth, 1977;
331 Russell *et al.*, 1979; Stucki *et al.*, 1984; Komadel and Stucki, 1990; Merola *et al.*, 2007; Stucki,

332 1988, 2006, 2013). The yellow-brown color of oxidized or unaltered CB-buffered Na-SWa-1
333 suspensions turned rapidly to green-yellow upon addition of sodium dithionite powder. With
334 time, the color changed progressively to green, blue-green, blue, blue-grey, and light grey, which
335 colors represented increasing structural Fe(II) content. Komadel and Stucki (1990) found that the
336 progression of these color changes, and hence of reduction, was enhanced by higher temperature
337 (70 °C) and by longer reaction time. They also found that the ideal dithionite:smectite ratio was
338 on the order of about 5:1 and that no further color change was observed after 4 h of the reduction
339 treatment at 70 °C. The grey color of the suspension, which occurs only in Fe-rich smectites,
340 indicated that reduction was finished.

341 These colors were also measured spectroscopically by monitoring the intervalence
342 electron transfer transition that occurs at about 730 nm in Fe-rich smectite (Figure 5). The
343 general trend in absorbance values with time of reduction was similar to that observed by
344 Komadel and Stucki (1990) for ferruginous smectite. The absorbance values at 0 and 4 h
345 represented the band intensities for the unaltered and maximum-reduced Na-SWa-1. The sample
346 at 4 h corresponded to samples prepared in the water bath at Stages 2 and 3. Because dithionite
347 was still in these suspensions, no attempt was made to analyze them chemically for Fe(II) and
348 total Fe, but they were analyzed by Mössbauer spectroscopy at 77 K (see below).

349 f_{295} were 0.821–0.917 for Fe³⁺ and 0.662–0.743 for Fe²⁺

- 350 • M. D. DYAR,
351 • M. W. SCHAEFER,
352 • E. C. SKLUTE,
353 • and J. L. BISHOP

354 Mössbauer spectroscopy of phyllosilicates: effects of fitting models on recoil-free
355 fractions and redox ratios *Clay Minerals*, March 2008, v. 43, p. 3-33, published online 1 April
356 2008,

357
358 Celadonite (from deGrave and van Alboom, 1991) gives $f_2 = 0.892$ and $f_3 = 0.935$, for a f_2/f_3
359 ratio of 0.954

360 $C_2/C_1 = k * A_2/A_3$ where $k=f_3/f_2$

361 $A_1/A_2 = C N_1/N_2$ where $C = a_1 b_1 f_1/a_2 b_2 f_2$ (see equation 3 and 4 of Dyar et al.)

362 Generally stated, $f_{3+} > f_{2+}$

363 Dyar found f_3 in nontronite and SWa1 to be 0.916 to 0.919, but no f_2 data.

364 Biotite gave $f_3 = 0.942$ and $f_2 = 0.871$ for a $f_2/f_3 = 0.924$

365

366 **Mössbauer Spectroscopy**

367 Na-SWa-1 reduced and treated up to Stage 3 was transferred to the Mössbauer sample
368 holder while inside the glove box, then the Mössbauer spectrum was obtained at 77 K (Figure 6).
369 Results revealed a sharp doublet characteristic of Fe(II) that accounted for 92.2% of the total
370 spectral area, with a small feature for Fe(III) accounting for the remaining area (7.8%),
371 indicating that the sample was highly reduced. This result is very close to the chemical analysis,
372 which found the Fe(II) content to be 91.129 % (± 0.477 %) of Total Fe (Table 2, Figure y). This
373 appears to be the maximum reduction level possible for ferruginous smectite.

374 After washing with the CALE (Stage 4), the spectrum (Figure 5) revealed that the Fe(III)
375 content increased only slightly to ?? % amount of Fe(III), and after freeze drying (Stage 5), the
376 spectrum had slightly more Fe(III) than before freeze drying. The corresponding values obtained

377 by chemical analysis were % and % (Figure y). The Mössbauer spectrum of a sample washed
378 without removing O₂ from the wash solutions (Stage 3b) revealed an increase in Fe(III) content
379 of about ?? %. These Mössbauer spectra were clear indicators that the methods employed to
380 prevent reoxidation were highly effective.

381 Stucki and co-workers (1984) observed a much lower level of Fe(III) conversion to Fe(II)
382 in C-B buffered Garfield nontronite suspensions at 25 °C than at 70 °C. Beside temperature, they
383 also studied the influence of sodium dithionite vs. clay loading and the reaction time on Fe
384 reduction level in Garfield nontronite. They reached the higher transformation of Fe from ferric
385 to ferrous oxidation state at 70 °C for 168 hours with loading 600 mg of sodium dithionite and
386 100 mg of the clay, respectively. In spite of strong conditions, the ratio of Fe(II):total Fe was ~
387 0.779 which was maybe caused by insufficient handling with the samples. The efficiency of our
388 developed procedure and improvement of presented a washing CALE apparatus for iron reduced
389 clay samples is in Table 1. Analysis of solid phases by 1, 10-phenanthroline method performed
390 10 times provided a high conversion level for 91.129 ± 0.477 % of Total Fe %, due to high
391 precise handling during reduce iron clay preparation.

392 CONCLUSIONS

393 Suspensions of Na-SWa-1 were reacted with sodium dithionite and buffered by sodium
394 citrate-sodium bicarbonate solution at 70 °C for 4 hours. Changes in color of unreacted and
395 reacted suspensions provided the clear evidence that iron in the clay structure was reduced. An
396 iron reductions under oxygen free conditions were performed with minimum Fe(II) back re-
397 oxidations to Fe(III). The proof of this argument was obtained from Fe(II) and total Fe
398 determination. Statistically, a transformation of the Fe(III) reduction to Fe(II) equals to $91.129 \pm$
399 0.477 % of Total Fe %. A controlled atmosphere liquid exchange (CALE) apparatus was

400 introduced and described in detail. Suitability of CALE apparatus for air sensitive iron clay
401 redox systems was demonstrated with success. It was effective in reaction products removal and
402 maintaining of high Fe reduction.

403

404 **REFERENCES**

- 405 Amonette, J.E. and Templeton, J.C. (1998) Improvements to the quantitative assay of non-
406 refractory minerals for Fe(II) and total Fe using 1,10-Phenanthroline. *Clays and Clay*
407 *Minerals*, **46**, 51-62.
- 408 Bishop, M.E., Dong, H., Kukkadapu R.K., Liu, C., and Edelman, R.E. (2011) Bioreduction of
409 Fe-bearing clay minerals and their reactivity toward pertechnetate (Tc-99). *Geochimica et*
410 *Cosmochimica Acta*, **75**, 5229-5246.
- 411 Cervini-Silva, J., Hernández-Pineda J., Rivas-Valdés, M.T., Cornejo-Garrido, H., Guzmán, J.,
412 Fernández-Lomelín, P., and Del Razo, L.M. (2010) Arsenic(III) methylation in betaine-
413 nontronite clay-water suspensions under environmental conditions. *Journal of Hazardous*
414 *Materials*, **178**, 450-454.
- 415 Dong, H.L., Kostka, J.E., and Kim, J. (2003) Microscopic evidence for microbial dissolution of
416 smectite. *Clays and Clay Minerals*, **51**, 502-512.
- 417 Dong, H.L., Kukkadapu, R.K., Fredrickson, J.K., Zachara, J.M., Kennedy, D.W., and
418 Kostandarithes, H.M. (2003) Microbial reduction of structural Fe(III) in illite and goethite.
419 *Environmental Science and Technology*, **37**, 1268-1276.
- 420 Dong, H.L., Jaisi, D.P., Kim, J., and Zhang, G.X. (2009) Microbe-clay mineral interactions.
421 *American Mineralogist*, **94**, 1505-1519.
- 422 Hofstetter, T.B., Schwarzenbach, R.P., and Haderlein, S.B. (2003) Reactivity of Fe(II) species
423 associated with clay minerals. *Environmental Science and Technology*, **37**, 519-528.
- 424 Jaisi, D.P., Kukkadapu, R.K., Eberl, D.D., and Dong, H. (2005) Control of Fe(III) site occupancy
425 on the rate and extent of microbial reduction of Fe(III) in nontronite. *Geochimica et*
426 *Cosmochimica Acta*, **69**, 5429-5440.

427 Jaisi, D.P., Dong, H.L., and Liu, C.X. (2007) Kinetic analysis of microbial reduction of Fe(III) in
428 nontronite. *Environmental Science and Technology*, **41**, 2437-2444.

429 Jaisi, D.P., Dong, H.L., Plymale, A.E., Fredrickson, J.K., Zachara, J.M., Heald, S., Liu, C.X.
430 (2009) Reduction and long-term immobilization of technetium by Fe(II) associated with
431 clay mineral nontronite. *Chemical Geology*, **264**, 127-138.

432 Komadel, P., and Stucki, J.W. (1988) Quantitative assay of minerals for Fe²⁺ and Fe³⁺ using
433 1,10-phenanthroline: III. A rapid photochemical method. *Clays and Clay Minerals*, **36**, 379-
434 381.

435 Komadel, P., Lear, P.R. and Stucki, J.W. (1990) Reduction and reoxidation of iron in
436 nontronites: Rate of reaction and extent of reduction: *Clays and Clay Minerals*, **37**, 203-208.

437 Komadel, P., Madejová, J., and Stucki, J. W. (1995) Reduction and reoxidation of
438 nontronites questions of reversibility. *Clays and Clay Minerals*, **43**, 105-110.

439 Komadel, P., Madejová, J., and Stucki, J.W. (2006) Structural Fe(III) reduction in smectites.
440 *Applied Clay Science*, **34**, 88-94.

441 Kostka, J. E., Wu, J., Nealson, K. H., and Stucki, J. W. (1999) The impact of structural Fe(III)
442 reduction by bacteria on the surface chemistry of smectite clay minerals. *Geochimica et*
443 *Cosmochimica Acta*, **63**, 3705-3713.

444 Kukkadapu, R.K., Zachara, J.M., Fredrickson, J.K., McKinley, J.P., Kennedy, D.W., Smith,
445 S.C., and Dong, H.L. (2006) Reductive biotransformation of Fe in shale-limestone saprolite
446 containing Fe(III) oxides and Fe(II)/Fe(III) phyllosilicates. *Geochimica et Cosmochimica*
447 *Acta*, **70**, 3662-3676.

448 Lee, K., Kostka, J.E., and Stucki, J.W. (2006) Comparisons of structural Fe reduction in
449 smectites by bacteria and dithionite: An infrared spectroscopic study. *Clays and Clay*
450 *Minerals*, **54**, 195-208.

451 Li, Y.L., Vali, H., Sears, S.K., Yang, J., Deng, B.L., and Zhang, C.L. (2004) Iron reduction and
452 alteration of nontronite NAu-2 by a sulfatereducing bacterium. *Geochimica et*
453 *Cosmochimica Acta*, **68**, 3251-3260.

454 Manceau, A., Lanson, B., Drits, V.A., Chateigner, D., Gates, W.P., Wu, J., Huo, D., and Stucki,
455 J.W. (2000) Oxidation-reduction mechanism of iron in dioctahedral smectites: I. Crystal
456 chemistry of oxidized reference nontronites. *American Mineralogist*, **85**, 133-152.

457 Manceau, A., Drits, V.A., Lanson, B., Chateigner, D., Wu, J., Huo, D., Gates, W.P., and Stucki,
458 J.W. (2000) Oxidation-reduction mechanism of iron in dioctahedral smectites: II. Crystal
459 chemistry of reduced Garfield nontronite. *American Mineralogist*, **85**, 153-172.

460 Merola, R.B., Fournier, E.D., and McGuire, M.M. (2007) Spectroscopic investigations of Fe²⁺
461 complexation on nontronite clay. *Langmuir*, **23**, 1223-1226.

462 Neumann, A., Hofstetter, T. B., Skarpeli-Liati, M., and Schwarzenbach, R. P. (2009) Reduction
463 of polychlorinated ethanes and carbon tetrachloride by structural Fe(II) in smectites.
464 *Environmental Science and Technology*, **43**, 4082-4089.

465 O'Reilly, S.E., Watkins, J., and Furukawa, Y. (2005) Secondary mineral formation associated
466 with respiration of nontronite, NAu-1 by iron reducing bacteria. *Geochem. Trans.*, **6**, 67-76.

467 O'Reilly, S.E., Furukawa, Y., and Newell, S. (2006) Dissolution and microbial Fe(III) reduction
468 of nontronite (NAu-1). *Chemical Geology*, **235**, 1-11.

469 Peretyazhko, T., Zachara, J.M., Heald, S.M., Jeon, B.H., Kukkadapu, R.K., Liu, C., Moore, D.,
470 and Resch, C.T. (2008) Heterogeneous reduction of Tc(VII) by Fe(II) at the solid-water
471 interface. *Geochimica et Cosmochimica Acta*, **72**, 1521-1539.

472 Ribeiro, F.R., Fabris, J.D., Kostka, J.E., Komadel, P., and Stucki, J. W. (2009) Comparisons of
473 structural iron reduction in smectites by bacteria and dithionite: II. A variable-temperature
474 Mössbauer spectroscopic study of Garfield nontronite. *Pure and Applied Chemistry*, **81**,
475 1499-1509.

476 Rozenson, I., and Heller-Kallai, L. (1976) Reduction and oxidation of Fe³⁺ in dioctahedral
477 smectite. I: Reduction with hydrazine and dithionite: *Clays and Clay Minerals*, **24**, 271-282.

478 Russell, J.D., Goodman, B.A., and Fraser, A.R. (1979) Infrared and Mössbauer studies of
479 reduced nontronites. *Clays and Clay Minerals*, **27**, 63-71.

480 Schaefer, M.V., Gorski, C.A., and Scherer, M.M. (2011) Spectroscopic evidence for interfacial
481 Fe(II)-Fe(III) electron transfer in a clay mineral. *Environmental Science and Technology*,
482 **45**, 540-545.

483 Southam, G. (2012) Minerals as substrates for life: The prokaryotic view. *Elements*, **8**, 101-105.

484 Stucki, J.W., and Roth, C.B. (1977) Oxidation-reduction mechanism for structural iron in
485 nontronite. *Soil Science Society of America Journal*, **41**, 808-814.

486 Stucki, J.W., and Anderson, W.L. (1981) The quantitative assay of minerals for Fe²⁺ and Fe³⁺
487 using 1,10-phenanthroline. I. sources of variability. *Soil Science Society of America Journal*,
488 **45**, 633-637.

489 Stucki, J.W. (1981) The quantitative assay of minerals for Fe²⁺ and Fe³⁺ using 1,10-
490 phenanthroline. II. A photochemical method. *Soil Science Society of America Journal*, **45**,
491 638-641.

492 Stucki, J. W. (2006) Properties and behavior of iron in clay minerals. Bergaya, F., Theng, B. K.
493 G., and Lagaly, G. (Eds.) Handbook of clay science. Elsevier, Amsterdam. pp. 429-482.

494 Stucki, J.W., and Tessier, D. (1991) Effects of iron oxidation state on the texture and structural
495 order of Na-nontronite gels. *Clays and Clay Minerals*, **39**, 137-143.

496 Stucki, J.W., Golden, D.C., and Roth, C.B. (1984a) Preparation and handling of dithionite-
497 reduced smectite suspensions. *Clays and Clay Minerals*, **32**, 191-197.

498 Stucki, J. W., Komadel, P., and Wilkinson, H.T. (1987) Microbial reduction of structural
499 iron(III) in smectites. *Soil Science Society of America Journal*, **51**, 1663-1665.

500 Stucki, J. W., Lee, K., Zhang, L. Z., and Larson, R. A. (2002) Effects of iron oxidation state on
501 the surface and structural properties of smectites. *Pure and Applied Chemistry*, **74**, 2145-
502 2158.

503 Zhang, G., Kim, J., Dong, H., and Sommer, A.J. (2007) Microbial effects in promoting the
504 smectite to illite reaction: Role of organic matter intercalated in the interlayer. *American
505 Mineralogist*, **92**, 1401-1410.

506 Zhang, G., Senko, J.M., Kelly, S.D., Tan H., Kemner, K.M., Burgos, W.D. (2009) Microbial
507 reduction of iron(III)-rich nontronite and uranium(VI). *Geochimica et Cosmochimica Acta*,
508 **73**, 3523-3538.

509 Zhuang, Y., Fialips, C.I., White, M.L., Perez Ferrandez, D.M. (2012) New redox-active material
510 for permeable water remediation systems. *Applied Clay Science*, **59–60**, 26-35.

511

512 **TABLE AND FIGURE CAPTIONS**

513 Table 1. The various configuration definitions for specific purposes of the CALE apparatus.

514 Figure 1. Schematic drawing of the CALE apparatus.

515 Figure 2. The details of the polycarbonate centrifugation tube (A) and the glass part (B) of a
516 CALE apparatus.

517 Figure 3. Schematic drawing of the Glove Box and Freeze Drying procedure.

518 Figure 4. The water jacked glass inert-atmosphere reaction tube (IRT).

519 Figure 5. A comparative iron analysis of the clay (SWa-1) samples washed with and without
520 CALE apparatus after dithionite reduction

521

522 **Table**

Configuration	A	B	C	D	E	F	G	H	I	J	K	L	M	N	O	P	Q	R
I. Filling flask with solution	Off/NA	Soln	1	1c	On	Off	1	3	On	Off	Off	Off	Off	Off	Down	NA	NA	NA
	Off/NA	Soln	2	2c	On	Off	2	3	On	Off	Off	Off	Off	Off	Down	NA	NA	NA
	Off/NA	Soln	3	3c	On	Off	3	3	On	Off	Off	Off	Off	Off	Down	NA	NA	NA
II. Deoxygenation of solution	Off/NA	Soln	4	4c	On	Off	4	3	On	Off	Off	Off	Off	Off	Down	NA	NA	NA
	1 [#]	Off	1/NA	1a [#]	Off	Off	1/NA	1	Off/On [~]	1 [#]	On	On	On	Off	NA	NA	NA	NA
	2 [#]	Off	2/NA	2a [#]	Off	Off	2/NA	1	Off/On [~]	2 [#]	On	On	On	Off	NA	NA	NA	NA
	3 [#]	Off	3/NA	3a [#]	Off	Off	3/NA	1	Off/On [~]	3 [#]	On	On	On	Off	NA	NA	NA	NA
III. Cool deoxygenated solution	4 [#]	Off	4/NA	4a [#]	Off	Off	4/NA	1	Off/On [~]	4 [#]	On	On	On	Off	NA	NA	NA	NA
	1 [#]	Off	1/NA	1a [#]	Off	Off	1/NA	1	Off	1	Off	On	On	On	NA	NA	NA	NA
	2 [#]	Off	2/NA	2a [#]	Off	Off	2/NA	1	Off	2	Off	On	On	On	NA	NA	NA	NA
	3 [#]	Off	3/NA	3a [#]	Off	Off	3/NA	1	Off	3	Off	On	On	On	NA	NA	NA	NA
IV. Store solution	4 [#]	Off	4/NA	4a [#]	Off	Off	4/NA	1	Off	4	Off	On	On	On	NA	NA	NA	NA
	Off/NA	Off	1/NA	1b	On	Off	1	3	On	Off	Off	Off	Off	Off	NA	NA	NA	NA
	Off/NA	Off	2/NA	2b	On	Off	2	3	On	Off	Off	Off	Off	Off	NA	NA	NA	NA
	Off/NA	Off	3/NA	3b	On	Off	3	3	On	Off	Off	Off	Off	Off	NA	NA	NA	NA
V. Decant and discard/save	Off/NA	Off	4/NA	4b	On	Off	4	3	On	Off	Off	Off	Off	Off	NA	NA	NA	NA
	Off/NA	Argon	NA	Off/NA	On	Discard	NA	3/NA	Off	Off	Off	Off	Off	Off	Up	Down	NA	NA
	Off/NA	Argon	NA	Off/NA	On	Save	NA	3/NA	Off	Off	Off	Off	Off	Off	Up	Down	Up	Up
	Off/NA	Soln	1	1c	On	either	1/NA	3	Off	1*	Off	Off	Off	Off	Up	Up	NA	NA
VI. Transport solution to the sample	Off/NA	Soln	2	2c	On	either	2/NA	3	Off	2*	Off	Off	Off	Off	Up	Up	NA	NA
	Off/NA	Soln	3	3c	On	either	3/NA	3	Off	3*	Off	Off	Off	Off	Up	Up	NA	NA
	Off/NA	Soln	4	4c	On	either	4/NA	3	Off	4*	Off	Off	Off	Off	Up	Up	NA	NA

[#] set an adequate flow rate
^{*} use this option in the case of insufficient solution flow rate
[~] use this option in the case of the solution outflow through the valve at the top of the condenser

- A: Condenser sweep
- B: Sample port
- C: Solution selection
- D: Feed to sample port – position a=Ar; position b=Off; position c=flask solution
- E: Main vacuum On or Off
- F: Decant selector, save or discard
- G: Vacuum to flask: selector
- H: Valve at the top of the condenser; position 1=all legs open; position 2=flask vented to right; position 3=flask closed
- I: Main vacuum to flask (on or off)
- J: Solution purge
- K: Hot Plate
- L: Stir Bar
- M: Condenser
- N: Cool Coil
- O: Needle 1, (from "Sample Port")
- P: Needle 2, (to "Decant Selector")
- Q: Needle 3, (from "Decant Selector")
- R: Needle 4, (to "Vacuum")

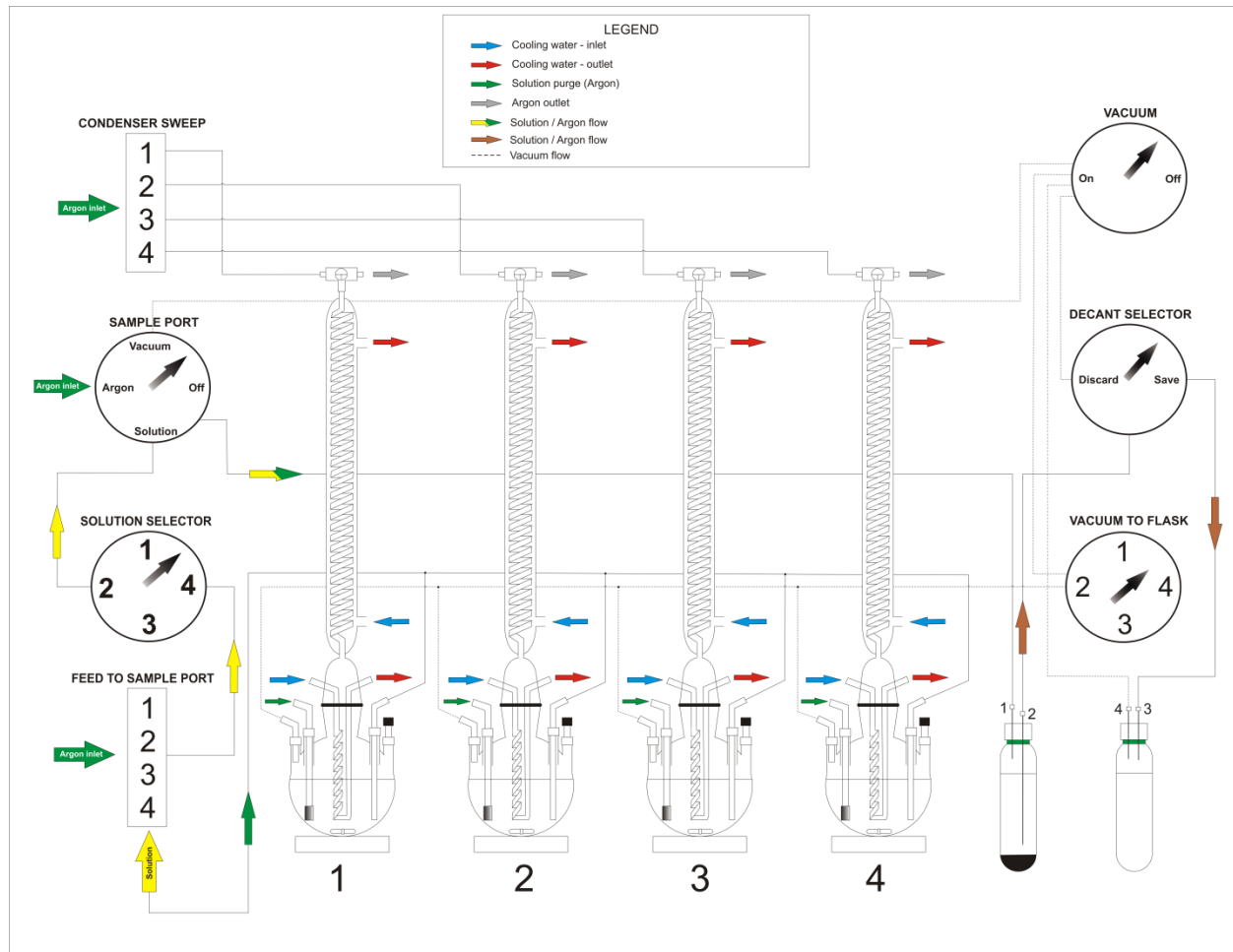
523

524

525

526 **Figures**

527 **Figure 1.**



528

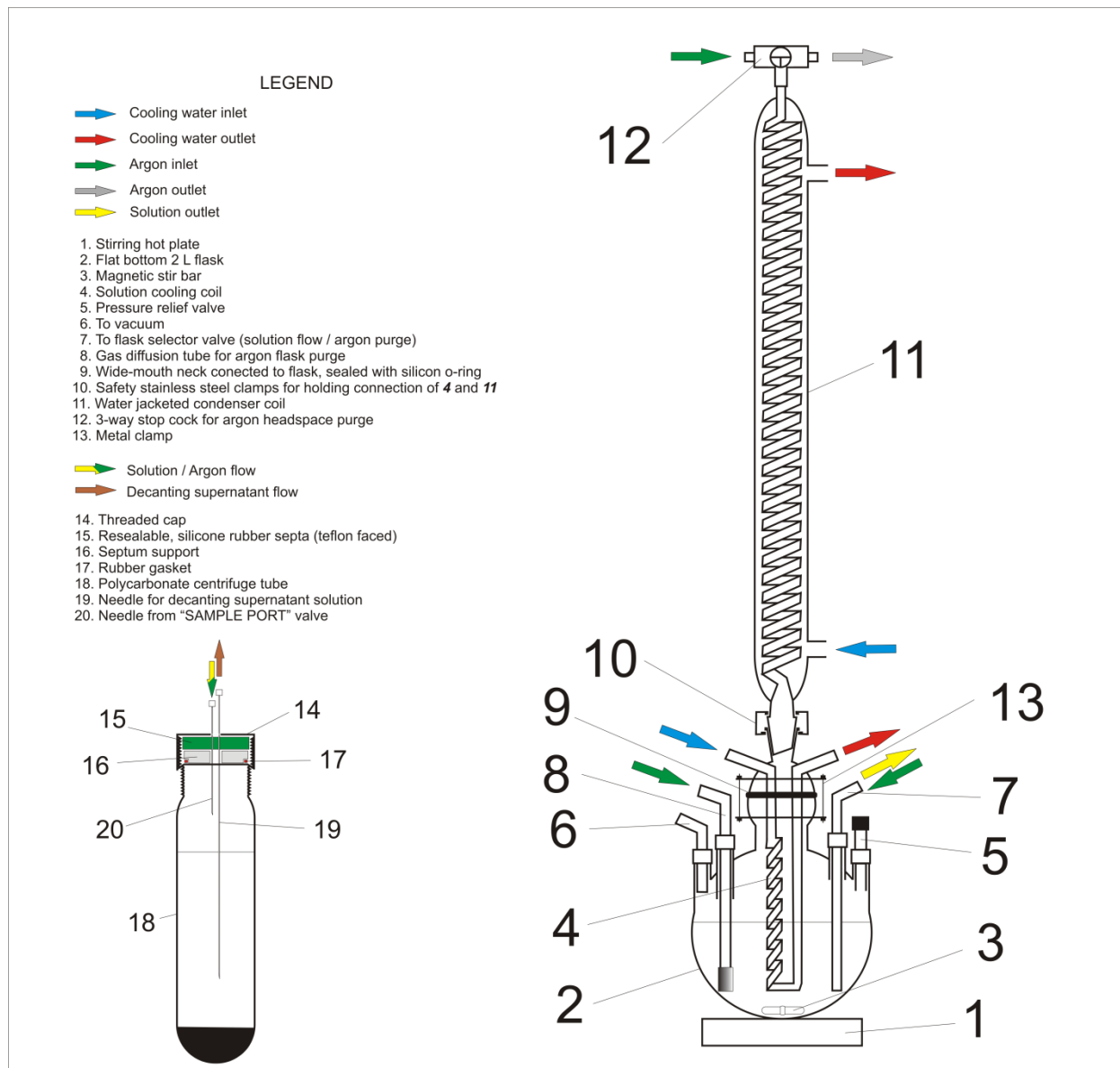
529

530

531

532

533



535

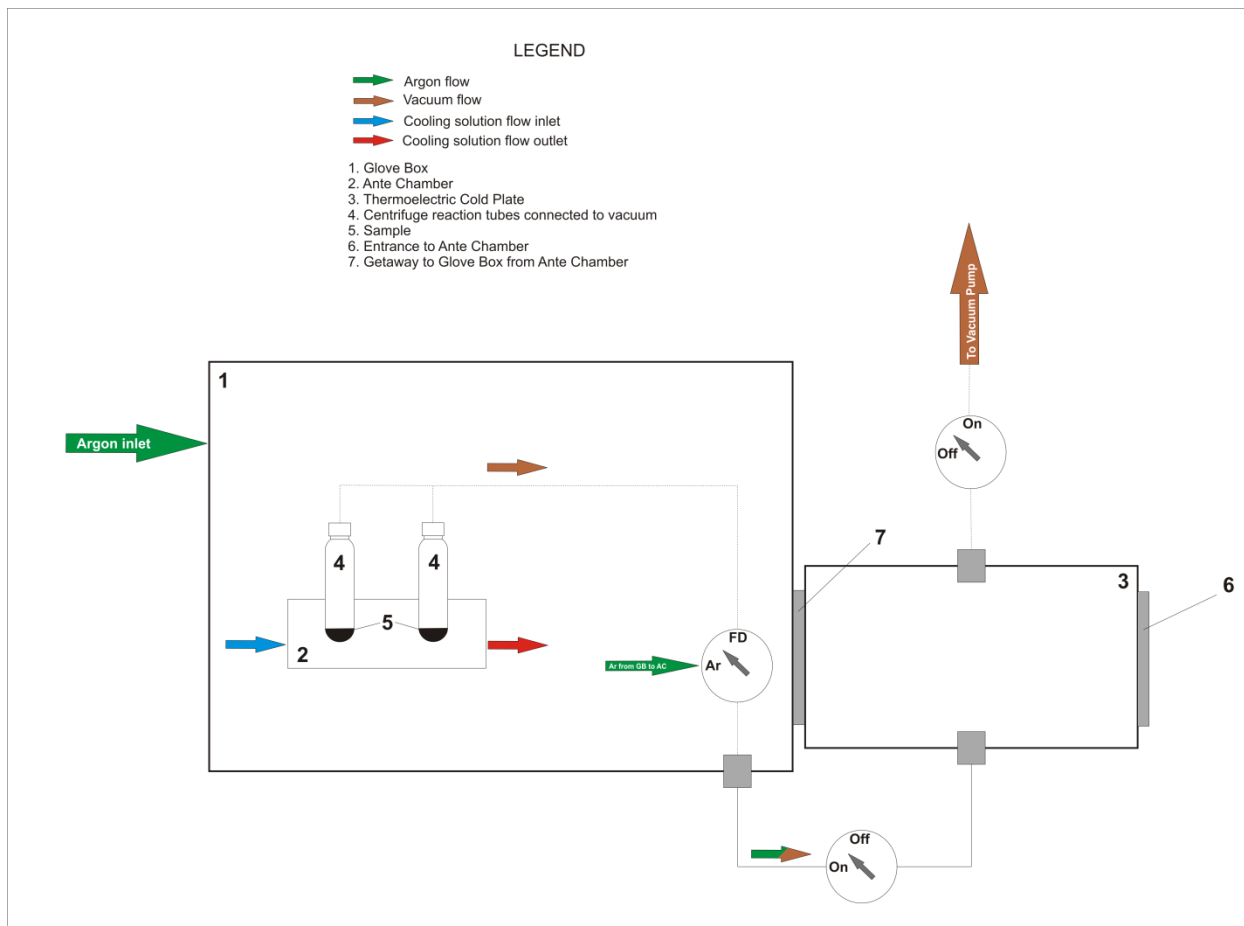
536

537

538

539

540 Figure 3.



541

542

543

544

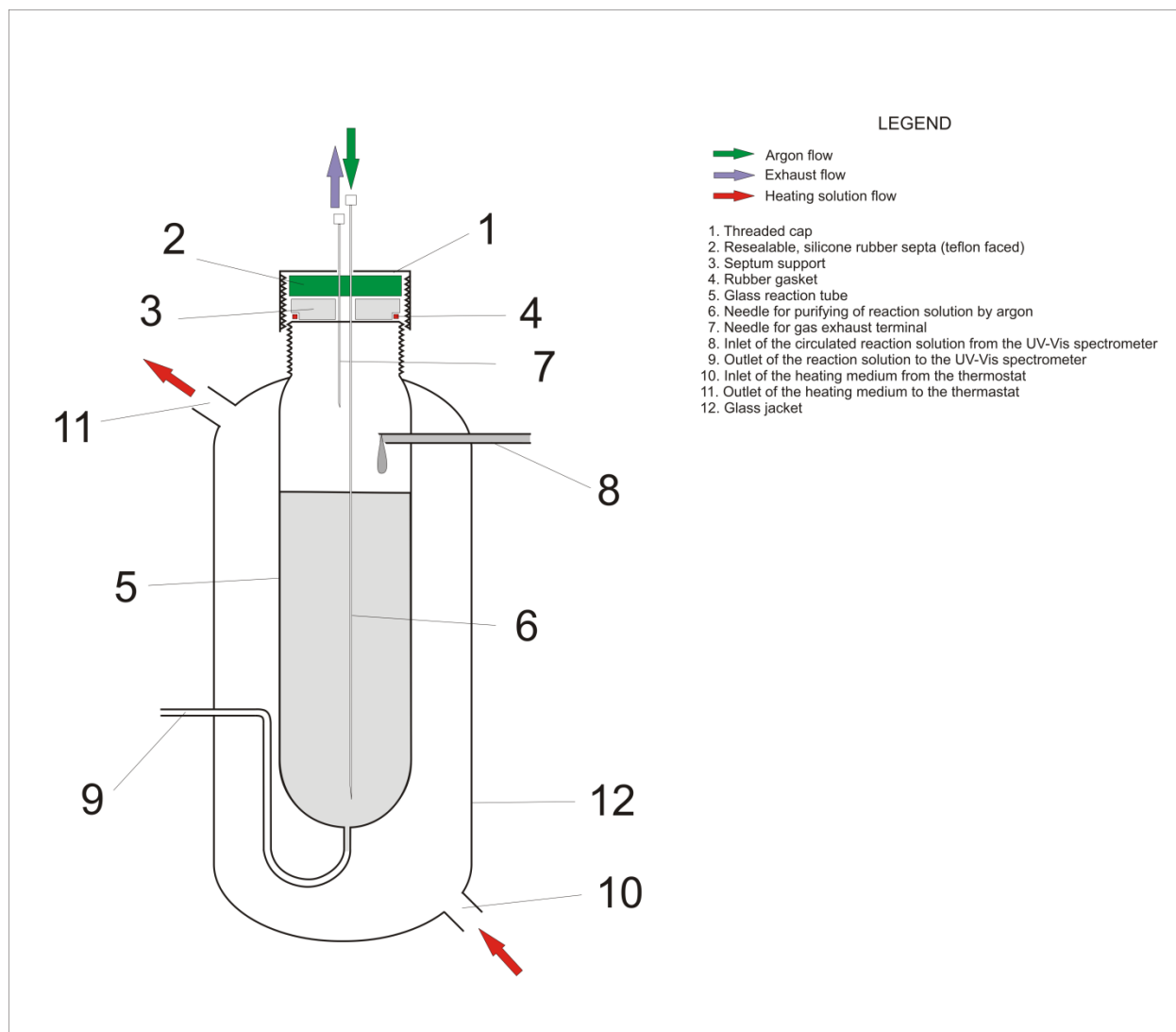
545

546

547

548

549 Figure 4.



550

551

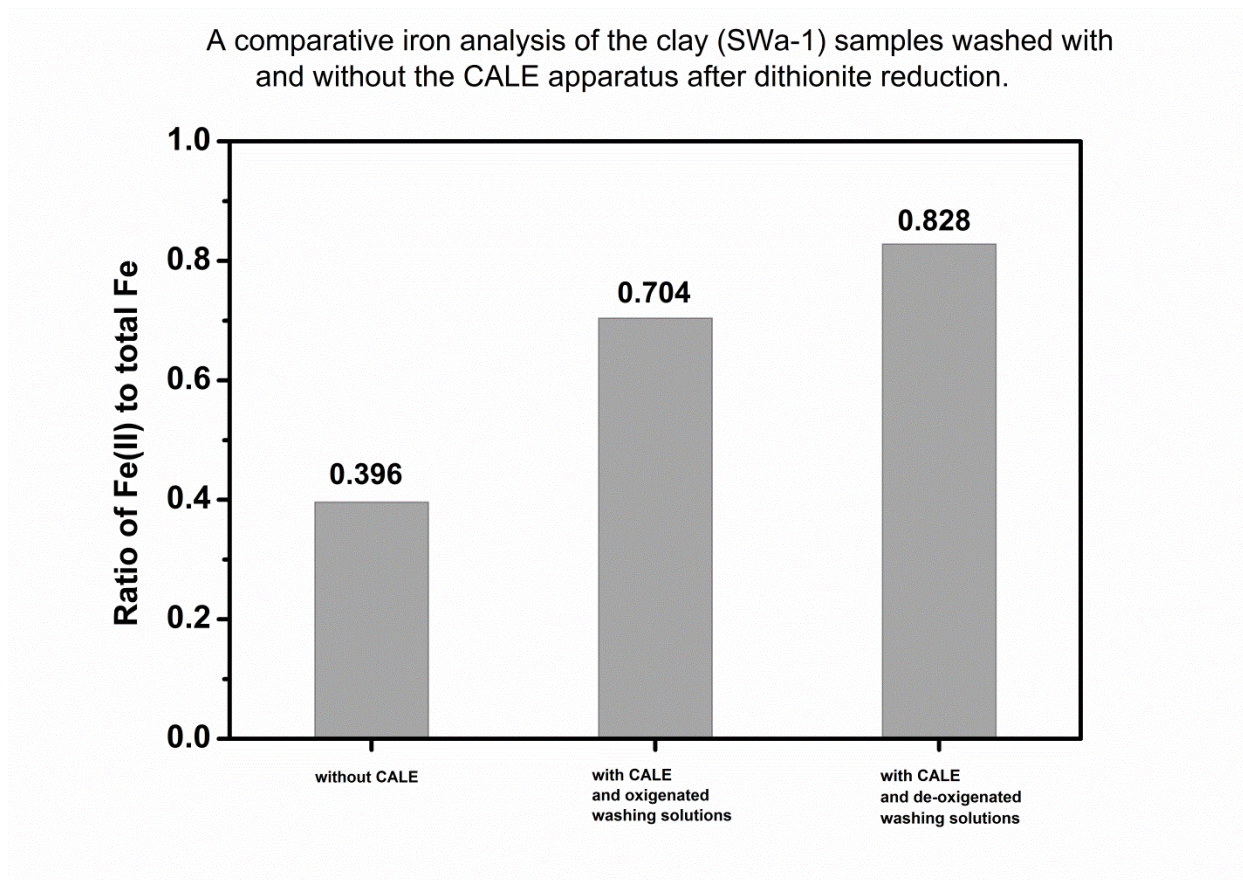
552

553

554

555

556 Figure 5.



557

558

559
560
561
562
563
564
565
566
567
568
569
570
571
572
573
574
575
576
577
578
579
580
581
582
583
584
585
586
587
588
589
590
591
592
593
594
595
596
597
598
599
600

REFERENCES CITED

- Alexandrov, V., Neumann, A., Scherer, M. M., and Rosso, K. M. (2013) Electron exchange and conduction in nontronite from first-principles. *Journal of Physical Chemistry C*, **117**, 2032-2040
- Dong, H., Jaisi, D. P., Kim, J., and Zhang, G. (2009) Microbe-clay mineral interactions. *American Mineralogist*, **94**, 1505-1519
- Gorski, C. A., Neumann, A., Sander, M., and Hofstetter, T. B. (2011) Assessing the redox properties of structural iron-bearing clay minerals using electrochemical and spectroscopic approaches. *Abstracts of Papers of the American Chemical Society*, **242**,
- Hofstetter, T. B., Neumann, A., Arnold, W. A., Hartenbach, A. E., Bolotin, J., Cramer, C. J., and Schwarzenbach, R. P. (2008) Substituent effects on nitrogen isotope fractionation during abiotic reduction of nitroaromatic compounds. *Environmental Science & Technology*, **42**, 1997-2003
- Komadel, P. and Stucki, J. W. (1988) Quantitative assay of minerals for fe-2+ and fe-3+ using 1,10-phenanthroline .3. A rapid photochemical method. *Clays and Clay Minerals*, **36**, 379-381
- Neumann, A., Petit, S., and Hofstetter, T. B. (2011) Evaluation of redox-active iron sites in smectites using middle and near infrared spectroscopy. *Geochimica Et Cosmochimica Acta*, **75**, 2336-2355
- Neumann, A., Hofstetter, T. B., Skarpeli-Liati, M., and Schwarzenbach, R. P. (2009) Reduction of polychlorinated ethanes and carbon tetrachloride by structural fe(ii) in smectites. *Environmental Science & Technology*, **43**, 4082-4089
- Neumann, A., Hofstetter, T. B., Lussi, M., Cirpka, O. A., Petit, S., and Schwarzenbach, R. P. (2008) Assessing the redox reactivity of structural iron in smectites using nitroaromatic compounds as kinetic probes. *Environmental Science & Technology*, **42**, 8381-8387
- Roth, C. B. and Tullock, R. J. 1972 Deprotonation of nontronite resulting from chemical reduction of structural ferric iron
- Roth, C. B., Jackson, M. L., and Syers, J. K. (1969) Deferration effect on structural ferrous-ferric iron ratio and cec of vermiculites and soils. *Clays and Clay Minerals*, **17**, 253-&
- Stucki, J. W. 1975 Chemical and spectroscopic analysis of oxidation-reduction mechanisms for structural iron in nontronite
- Stucki, J. W. (1981) The quantitative assay of minerals for fe²⁺ and fe³⁺ using 1,10-phenanthroline .2. A photochemical method. *Soil Science Society of America Journal*, **45**, 638-641
- Stucki, J. W. (2006) Properties and behavior of iron in clay minerals. Bergaya, F., Theng, B. K. G., and Lagaly, G. (Eds.) *Handbook of clay science*. Elsevier, Amsterdam. pp. 429-482.
- Stucki, J. W. (2013) Properties and behaviour of iron in clay minerals. Bergaya, F. and Lagaly, G. (Eds.) *Handbook of clay science*. Elsevier, Amsterdam. pp.
- Stucki, J. W. and Roth, C. B. (1977) Oxidation-reduction mechanism for structural iron in nontronite. *Soil Sci. Soc. Am. J.*, **41**, 808-814
- Stucki, J. W. and Anderson, W. L. (1981) The quantitative assay of minerals for fe²⁺ and fe³⁺ using 1,10-phenanthroline .1. Sources of variability. *Soil Science Society of America Journal*, **45**, 633-637
- Violet, C. E. and Pipkorn, D. N. (1971) Mossbauer line positions and hyperfine interactions in alpha iron. *Journal of Applied Physics*, **42**, 4339-&

Wu et al., 1989

601

602 With the cooling coil 8 and condenser 10 removed from the flask, the washing solution
603 was poured into the flask through the wide mouth 9, then 8 and 10 were joined together by a
604 standard-taper, ground-glass joint and 8 was attached to the wide-mouth joint 9 of the flask using
605 an o-ring and metal clamp. Cold tap water was circulated continuously through the outer jacket
606 of condenser column 10 and O₂-free Ar gas was swept through the 3-way valve 11 across the top
607 of column 10, with the valve also open to the flask. Oxygen-free Ar was then admitted into the
608 solution through gas dispersion tube 5 by the proper setting of the 3-way valve A (Figure 6,
609 “Feed to sample port”) was opened so Ar sweep gas solution was then deoxygenated by then the
610 cooling coil on a stirring hot plate (Fig.3, B-2) equipped with a magnetic stir bar (Fig.3, B-3). A
611 condenser coil (Fig.3, B-8) is attached to the central neck of each flask, which is used for rapid
612 cooling of the solution after boiling. Above the whole flask at the central neck is a water jacketed
613 condenser column for total reflux of boiling solution (Fig.3, B-9). Oxygen-free argon inlet
614 controlled by 3-way valve “Feed to sample port” and loaded to the one of four little threaded
615 necks (Fig.3, B-5) passed through solution via gas dispersion tube and solutions were boiled
616 approximately 1 hour with stirring, because the solubility of the gases in the water decreases with
617 increasing temperature. The 3-way valve (Fig.3, B-10) at the top of reflux cooler was opened to
618 secure outlet exhaust and avoid increase of pressure in the flasks. The stopcock was closed after
619 the solutions had been cooled and some solution was passed via solution outlet (Fig.3, B-6). The
620 little threaded neck (Fig.3, B-7) is equipped with the pressure relief valve (10 PSI) for safety and
621 during all operations of the CALE apparatus must be covered by the transparent safety shield
622 (Fig.1).

623 The IRT containing the freshly reduced, cooled Na-SWa-1 was centrifuged (Sorvall
624 Dupont Model RC4-M Plus centrifuge with SS-33 rotor) at 5000 rpm which corresponds to 3000

625 x g (Martin, please confirm this rpm and calculate the corresponding g force), then the
626 supernatant solution was decanted and replaced with 1 M NaCl from flask 1 (Figure 1 and Figure
627 4). This washing step was repeated three to five more times using 0.005 M NaCl from flask 2.
628 After the last washing step with NaCl, DI water was added from flask 3. The figure 3 shows
629 details of the reaction centrifugation tube (A) and the glass part of CALE apparatus (B).

630 Prior to washing steps the samples were centrifuged for 15 minutes at 1400 x g with the
631 SS-34 rotor on the Dupont Sorvall Model RC 5C plus. In the case of insufficient dispersion
632 presence (supernatant occurs cloudy) the double centrifuge speed is needed. When the
633 supernatants were clear and washing solutions properly deoxygenated, the decanting of the
634 supernatants was performed by CALE without exposure to the atmosphere. Two septum
635 penetration needles are inserted into to the centrifugation tubes (Fig.3, A-11) via silicon rubber
636 septa. The needles were designed with the tip in the side wall for penetration without coring a
637 hole. The needle (Fig.3, A-12) lowered into the clear supernatant solution one cm above
638 sediment in the bottom for decanting the supernatant solution, which feeds through the Tygon
639 tube into a large neck filter flask under vacuum. The needle (Fig.3, A-13) inserted about one cm
640 through the septa cap. This needle is attached to a 4-way valve "SAMPLE PORT". In position
641 "OFF" the needle is closed. In position "Argon" is used for pumping the O₂-free Argon into the
642 centrifuge tube to enhance the pressure gradient for the supernatant solutions removal support
643 and to prevent negative pressures inside the tube and feeding a new washing solution from
644 selected bottom rounded flasks (Fig.3, B-1). In position "VACUUM" the needle can be used as a
645 vacuum needle. In position "SOLUTION" the needle is connected to a 4-way valve
646 "SOLUTION SELECTOR" which allows inflow of the fresh deoxygenated solution from the
647 selected flasks (Fig.1).

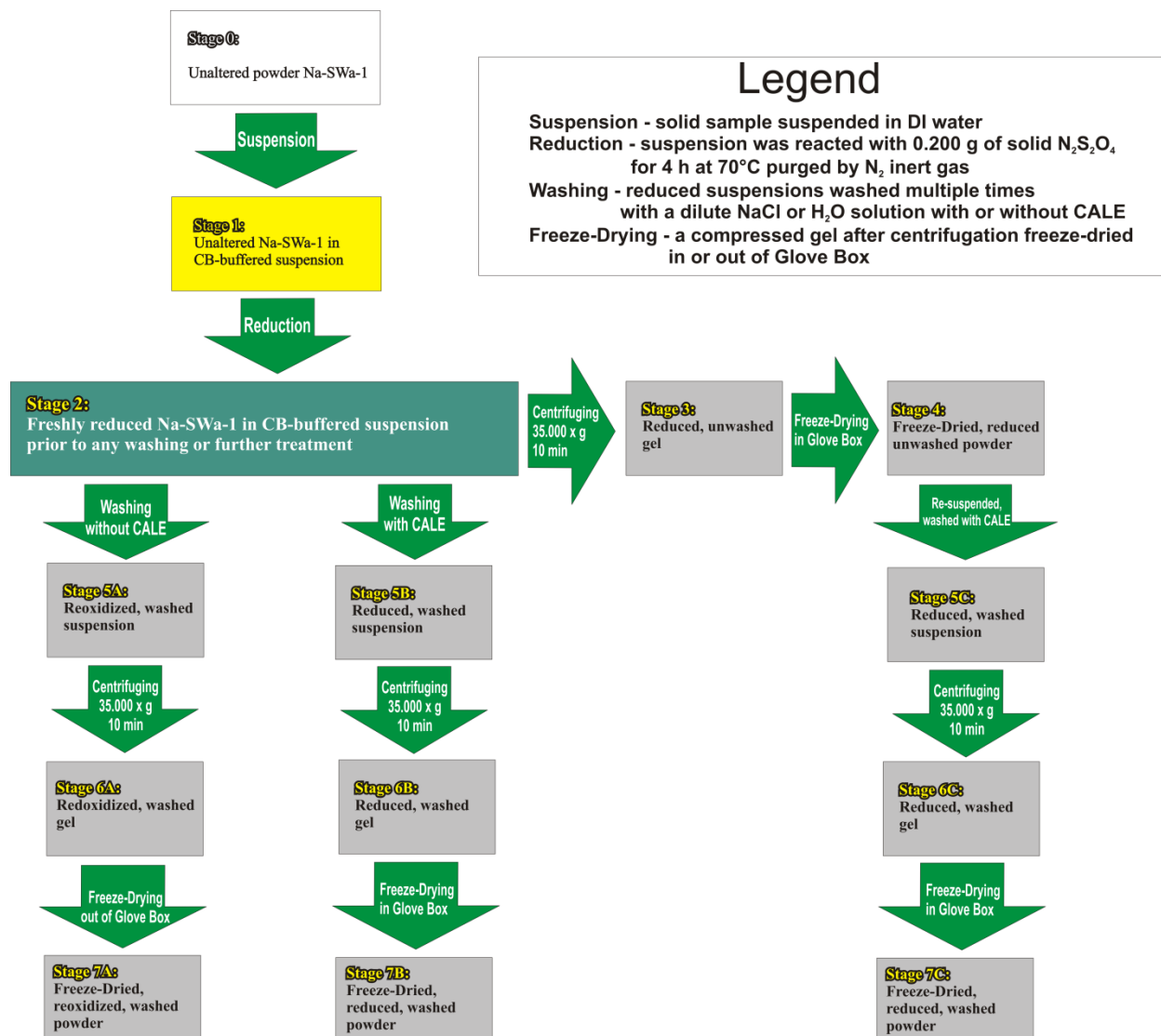
648 Once “the needle to vacuum” (Fig.3, A-12) is inserted into the centrifugation tube
649 through the green silicon septa the supernatant is vacuumed and the pressure in the reaction tube
650 getting low. This deficit must be compensated by incoming argon provided by “the needle from
651 the flask” (Fig.3, A-13), connected to the 4-way valve “SAMPLE PORT” which is set to
652 “Argon” position (Fig.1 and Fig.4). The supernatant is removed and fresh deoxygenated washing
653 solution of 1 mol.dm⁻³ NaCl is not added, leaving a small amount of reduced clay in an
654 atmosphere of argon within the tube and “the needle to vacuum” retrieved 1 cm under silicon
655 septum for the fresh washing solution income enhancing. At need, the extracted solutions can be
656 saved or wasted, the “DECANT SELECTOR” valve in position “SAVE” or “DISCARD”,
657 respectively. The three steps to get washing solutions inside the reaction tubes are needed.
658 “FEED TO SAMPLE PORT” adjusted to “FLASK 1” position, “SOLUTION SELECTOR” in
659 position “1” and “SAMPLE PORT” in position “SOLUTION”, provided the O₂-free 1 mol.dm⁻³
660 NaCl solution flowing to the centrifugation tube. When the required volume of fresh solution is
661 reached, “the needle to vacuum” is released and the “SAMPLE PORT” is switched to “OFF”
662 position (Fig.1 and Fig.4).

663 Prepared oxygen sensitive redox samples for storage should be placed into the main
664 store-room via antechamber for next use. The first be sure that gateway between the main store
665 and antechamber is closed securely. Then the right door can be opened and samples placed to
666 sliding tray and immediately closed to prevent oxygen penetration into the glove box (Fig.6).
667 Now the glove box should be purged by Nitrogen and Oxygen in antechamber removed. The air
668 from the antechamber will be evacuated by “EVACUATION VALVE” till the vacuum reaches -
669 100 in Hg. When the “EVACUATION VALVE” is closed, the automatic pressure control will
670 start fill the glove box and the red LODs are moved to the left – maximum gas filling. When the

671 orange LEDs indicate an over-pressure, the “REFILL VALVE” must be opened. The Nitrogen
672 from the main store-room starts taking place in the antechamber and the manometer indicates the
673 pressure increasing till + 30 inHg. The pressure in the glove box must never go to the right.
674 When this limit is reached, the “REFIL VALVE” must be closed and “EVACUATION VALVE”
675 opened. To reach the total oxygen replacement for nitrogen in the glove box, this procedure
676 should be repeated for four times. In case of many samples or material placed in the
677 antechamber, the “refilling & evacuating” cycles must by repeated five times or more, due to
678 larger amount of oxygen trapped inside and risks bringing too much oxygen inside. The common
679 operating conditions inside the glove box, the pressure on the automatic pressure control system
680 is set to + 2 in water (red LEDs). After the purging cycles have been completed, the door
681 between the main store-room and the antechamber can be opened and the samples removed from
682 the sliding tray and deposited inside the main store-room.

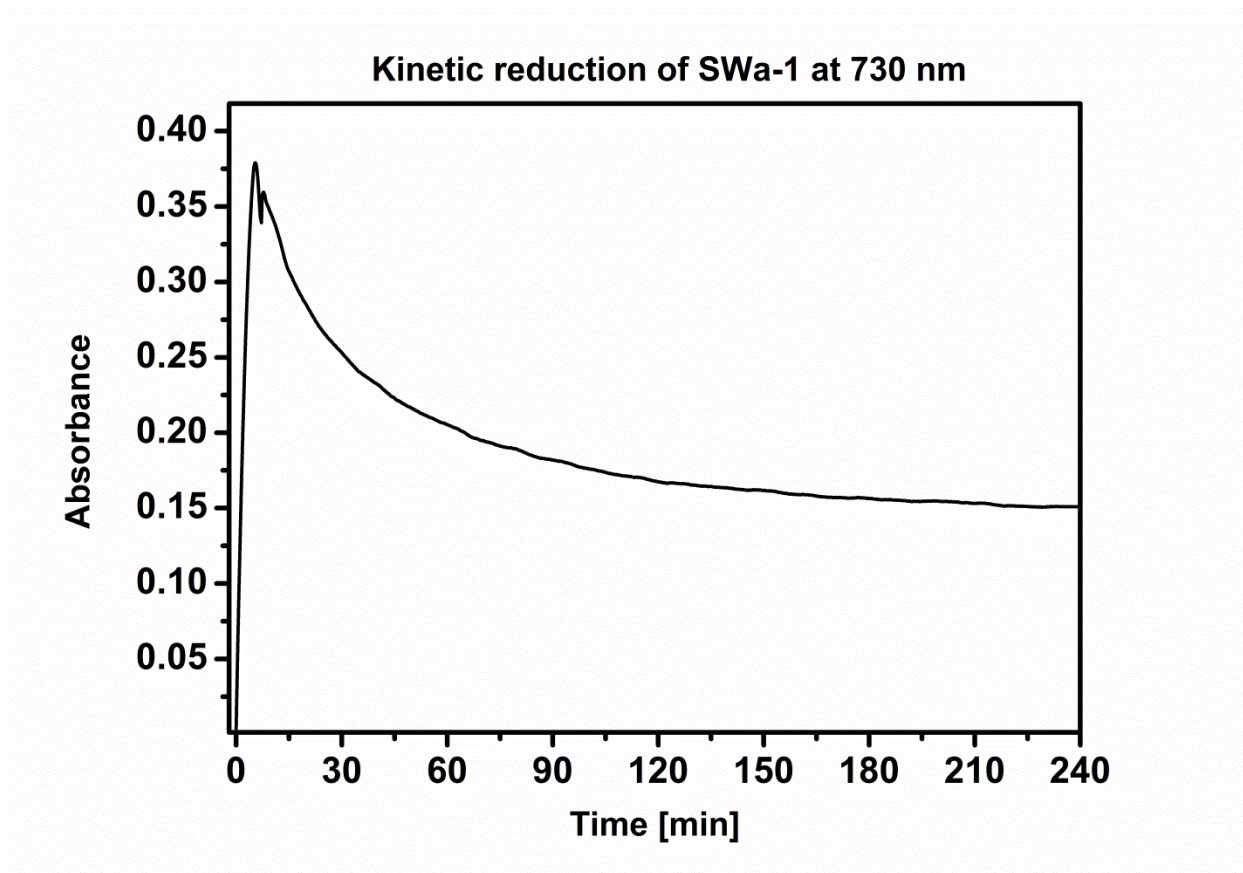
683

684



685

686



687

688 Figure 5. Intervalence electron transfer transition intensity (Absorbance) of structural Fe in
689 SWa-1 with time of exposure to dithionite at 70 °C.

690

691 consisted of three essential features: (1) Several condenser flasks placed on stirrer hot
692 plates in which selected solutions were deoxygenated; (2) a distribution and control network
693 consisting of valves, fittings, and tubing to connect the IRT with selected flasks, decanting
694 circuits, O₂-free gas supplies, and vacuum, and to connect the flasks with O₂-free gas supplies
695 and vacuum; and (3) a housing in which the flasks were placed to protect the operator from
696 accidental glass breakage and to support the distribution and control network with a comfortable
697 operator interface and work station (Figure 2).

698